arXiv:1608.04957v2 [cond-mat.supr-con] 7 Sep 2016

Size Dependence of Oxygen-annealing Effects on Superconductivity of $Fe_{1+y}Te_{1-x}S_x$

Teruo Yamazaki, Tatsuya Sakurai, and Hiroshi Yaguchi

Department of Physics, Faculty of Science and Technology, Tokyo University of Science, Noda, Chiba 278-8510, Japan

For the Fe-based superconductor $Fe_{1+y}Te_{1-x}S_x$, superconductivity is induced by annealing treatment in oxygen atmosphere, whereas as-grown samples do not show superconductivity. We have investigated the sample-size dependence of O_2-annealing effects in $Fe_{1.01}Te_{0.91}S_{0.09}$. The annealing conditions are fixed to be 1 atm, 200 °C, and 2 hours. We have carried out magnetic susceptibility and specific heat measurements in order to evaluate the superconducting volume fraction. We have found that $Fe_{1+y}Te_{1-x}S_x$ has an optimal size for the induction of bulk superconductivity by O_2 annealing. Our results indicate that O_2 annealing is probably effective near the surface of samples over a length of a few tens of micro meters.

1. Introduction

Numerous iron-based superconductors have been reported since the discovery of superconductivity in LaOFeP and $La(O_{1-x}F_x)FeAs$.[1,2] Among them, iron chalcogenide materials such as FeSe, $Fe_{1+y}Te_{1-x}Se_x$, and $Fe_{1+y}Te_{1-x}S_x$ are categorized as 11-systems.[3] The 11-system attracts researchers' attention because of the simplest crystal structure. The crystal structure of $Fe_{1+y}Te$ is tetragonal and the space group is $P4/nmm$. $Fe_{1+y}Te$ ($y \leq 0.12$) does not show superconductivity, but exhibits a structural phase transition to a monoclinic ($P2_1/m$) phase at $T_s \sim 65$ K. The transition is accompanied by a magnetic phase transition to a commensurate antiferromagnetic phase with a wave vector of $\boldsymbol{q} = \left(\frac{1}{2}, 0, \frac{1}{2}\right)$. In the higher iron concentration range of $y \geq 0.12$, tetragonal $Fe_{1+y}Te$ undergoes a structural phase transition to an orthorhombic ($Pmmn$) phase and a magnetic phase transition with an incommensurate magnetic structure with $\boldsymbol{q} = \left(\pm\delta, 0, \frac{1}{2}\right)$, where $\delta = 0.38$ for $Fe_{1.141}Te$.[4–8] The substitution of S for Te in $Fe_{1+y}Te$ suppresses the structural and the magnetic phase transition temperatures. While as-grown samples of $Fe_{1+y}Te_{1-x}S_x$ exhibits no superconductivity for all the compositions of x and y,[9] superconductivity can be induced in $Fe_{1+y}Te_{1-x}S_x$ by several kinds of treatments. Examples of such treatments are leaving in the air for a long time,[10] annealing in O_2 atmosphere

(O_2 annealing),[11–13] annealing in S atmosphere,[14] and soaking in hot alcoholic beverages or aqueous organic solutions, e.g. red wine or malic acid.[15,16] After the soaking treatment in the aqueous organic solutions, an Fe component has been detected in the solutions.[16] Hence, it is inferred that the deintercalation of excess Fe may be a key for the induction of superconductivity in $Fe_{1+y}Te_{1-x}S_x$.

In another 11 system, $Fe_{1+y}Te_{1-x}Se_x$, superconductivity can be also induced by various treatments.[14,17–21] Among the treatments, annealing in low-pressure oxygen atmosphere or in vacuum can induce bulk superconductivity, and a large critical current density J_c and a discontinuity of the specific heat have been observed.[17,18,20] By contrast, no evidence for bulk superconductivity in $Fe_{1+y}Te_{1-x}S_x$ has been observed thus far, although zero electrical resistivity and large diamagnetic susceptibility in zero-field-cooled (ZFC) condition have been observed in $Fe_{1+y}Te_{1-x}S_x$ samples after similar treatments. Therefore, it is speculated that the superconducting state could be realized only within particular regions of the samples.

In the present work, we have investigated the sample-size dependence of the O_2-annealing effects by means of ZFC and field-cooled (FC) susceptibility and specific heat measurements. We have chosen the O_2-annealing condition to be 1 atm, 2 hours, and 200 °C, following Ref. 11. We observed a jump of the specific heat around the superconducting transition temperature T_c in relatively small O_2-annealed samples. To the best of our knowledge, this is the first observation of bulk superconductivity in $Fe_{1+y}Te_{1-x}S_x$. We deduce that the superconducting region induced by O_2 annealing is probably near the surface of samples over a length of a few tens of micro meters.

2. Experimental Procedure

The single crystalline samples of $Fe_{1+y}Te_{1-x}S_x$ used in the present study were prepared by a self flux method described in Ref. 9. Fe shot (5N), Te shot (6N), and S shot (6N) with a nominal composition of $x = 0.2$ were sealed in evacuated quartz ampoule under atmosphere of 0.3-atm argon. The ampoule was heated by an electric furnace to 1050 °C. Subsequently, the temperature was kept for 20 hours and then cooled to 650 °C at a rate of −4 °C / h. All the samples used in this work were obtained from the same batch. The dimensions of the single crystalline sample for measurements were $3\,\mathrm{mm} \times 3\,\mathrm{mm} \times 0.5\,\mathrm{mm}^3$ (class #1). We prepared powder samples by crushing single crystals, and classified them by size using sieves into the following dimensions; 106–250 μm (class #2), 75–106 μm (class #3), 20–75 μm (class #4), and 0–20 μm (class #5). The samples were annealed in O_2 atmosphere . The pressure, temperature, and duration for the O_2 annealing were fixed to be 1 atm, 200 °C, and 2 hours,

respectively.

The actual composition of the samples were determined to be $Fe_{1.01}Te_{0.91}S_{0.09}$ using an electron probe micro analyzer EPMA (JEOL, JXA-8100). X-ray powder diffraction measurements with Fe-K_α radiation were performed using RIGAKU, RAD-C.

We measured the magnetic susceptibility using a superconducting quantum interference device (SQUID) magnetometer (Quantum Design, MPMS). For the magnetic susceptibility measurements, the applied field was 20 Oe. The single crystalline sample (sample class #1) was mounted in a plastic straw so that the applied field is along the longest dimension. The powder samples (sample class #2–#5) were wrapped in cling film and mounted in plastic straws. We have also measured the specific heat by a thermal relaxation method (Quantum Design, PPMS). For specific heat measurements for class #3 (75–106 μm), the sample was wrapped in copper foil; the heat capacity and the specific heat of the samples were evaluated by subtracting the heat capacity of the copper foil as described in Ref. 22. For the subtraction, the data of the specific heat measured for copper in Ref. 23 were used. For the other samples, pellets, prepared by pressing small pieces of crystals, were used for specific heat measurements. The samples used for magnetic susceptibility, specific heat, and X-ray diffraction measurements are labeled with a, b, and c, respectively, preceded by the class number, e. g. sample 1a.

3. Experimental Results

Figures 1(a) and (b) show the temperature dependences of the superconducting shielding fraction (SF) of size-classified O_2-annealed $Fe_{1.01}Te_{0.91}S_{0.09}$ evaluated from the magnetic susceptibility, $\Delta\chi(T) = \chi(T) - \chi(15\,\mathrm{K})$, measured (a) in the zero-field-cooled (ZFC) condition and (b) field-cooled (FC) condition. In this work, the demagnetizing field effects are ignored. The onset of the superconducting transition temperature (onset T_{c1}) for single crystalline sample 1a is 8.8 K, and the onset T_{c1} rises to 9.4 K for the powder samples. The inset of Fig. 1(b) depicts an example of the definition of the onset T_c. The SF at 5 K for sample 1a in the ZFC condition is 12%. and the SF at 5 K for samples 2a–4a (20–250 μm) is enhanced and is over 80% in the ZFC condition. For the smallest sample 5a (0–20 μm), however, the SF is suppressed to 14% at 5 K. On the other hand, the SF in the FC condition for sample 1a (single crystal) is only about 1%. The SF in the FC condition increases with decreasing sample size except for sample 5a. For sample 5a, the SF in the FC condition is only 1%. The SF measured in the FC condition is correlated with the superconducting volume fraction (SVF). Accordingly, we use the SF in the FC condition as a measure of the SVF. The sample-size

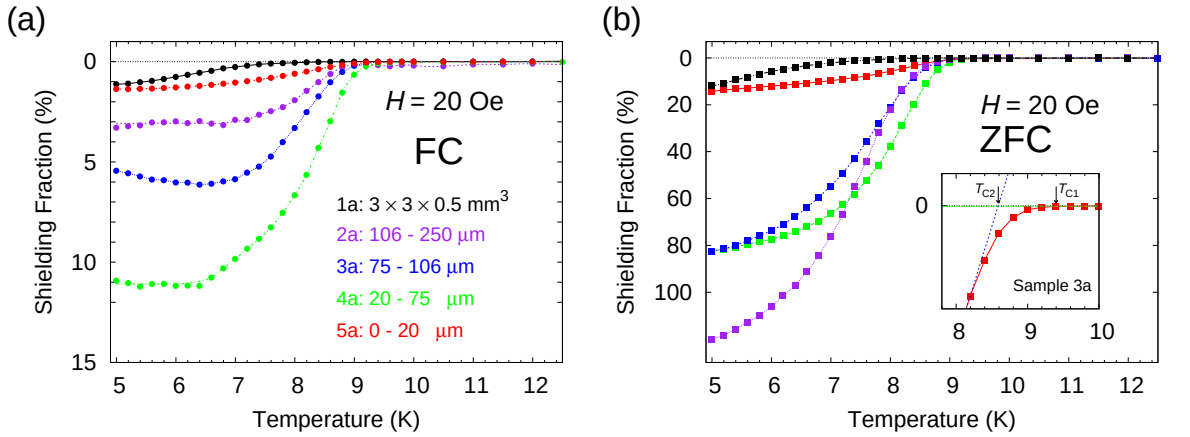

Fig. 1. (Color online) Temperature dependences of shielding fraction (SF) in O_2-annealed $Fe_{1.01}Te_{0.91}S_{0.09}$. Inset shows an example of the definition of onset T_{c1} and onset T_{c2} for sample 3a. Onset T_{c1} is defined by the start point of the drop of the magnetic susceptibility. Onset T_{c2} is defined by the intersection of the straight fitting line of the superconducting region with that of the normal state region.

dependence of the SF measured in the FC condition is summarized in Table I. The results indicate that the O_2-annealing effects for the $Fe_{1+y}Te_{1-x}S_x$ strongly depends on the sample size, and there appears to be an optimum sample size to maximize the SVF.

Table I. Shielding fraction at 5 K in the FC condition (SF-FC) and onset T_{c1} and onset T_{c2} defined in Fig. 1.

Sample	size	SF-FC (%)	onset T_{c1} (K)	onset T_{c2} (K)
1a	3 3 0.5 mm^3	1.1	8.8	7.0
2a	106–250 μm	3.2	9.4	8.4
3a	75–106 μm	6.2	9.4	8.6
4a	20–75 μm	11.0	9.4	8.8
5a	0–20 μm	1.2	9.2	8.9

The specific heat provides quantitative and reliable information about the SVF. The specific heat divided by temperature, C/T, against T^2 is plotted in Fig. 2 (a). Peaks associated with the superconducting transition were observed in the O_2-annealed powder samples 2a - 5a, although such a peak was hardly observed in the single crystalline sample 1b. As will be described later, these samples used include several kinds of impurities, e. g. $FeTe_2$. It is, therefore, difficult to distinguish the specific heat of $Fe_{1.01}Te_{0.91}S_{0.09}$ from those of the impurities. Here we analyze the specific heat data assuming the following simple formula for the temperature range of $100\,K^2 \le T^2 \le 196\,K^2$,

$$\frac{C}{T} = \gamma + \beta T^2, \tag{1}$$

where γ and β mainly come from the electronic and the lattice specific heat coefficients of $Fe_{1.01}Te_{0.91}S_{0.09}$, respectively. Figure. 2(b) shows the electronic part of the specific heat obtained from the data on the assumption of the functional form of equation (1). This analysis apparently fails to extract the electronic contribution of $Fe_{1.01}Te_{0.91}S_{0.09}$ because the entropy balance is not conserved in Fig. 2(b). Nevertheless, the peaks observed in the specific heat are so clear that their attributions to the superconducting transition appear to be plausible. The onset temperature of the peak (onset T_c), the peak temperature (T_c^{peak}), and the parameters obtained from the fitting procedure are tabulated in Table II. Note that fitting the experimental data to equation (1) yields γ and β including the contributions from the impurities. The Debye temperature θ_D estimated from β in sample 1b is 149 K, which is close to a Debye temperature of 141 K for the parent compound $Fe_{1.05}Te$ reported in Ref.24. The onset temperature of the peak increases to about 10.2 K with decreasing sample size for samples 2b–4b and that of sample 5b slightly decreases. The peak temperature is about 8.0 K in the sample 2b–5b. The peak heights $\Delta C/T_c^{peak}$ of samples 3b and 4b are very close (31 mJ/Fe-mol K^2) and are the greatest among the samples.

The size dependence observed in the susceptibility and the specific heat measurements indicates that the O_2 annealing affects due to the distance from surface. To identify the materials created in the samples through O_2 annealing, X-ray diffraction measurements were carried out. Figure 3(a) shows the X-ray diffraction patterns of size-classified O_2-annealed samples of $Fe_{1.01}Te_{0.91}S_{0.09}$, and those of an as-grown sample for comparison. While the as-grown sample was ground for the measurements, the O_2-annealed samples were mounted on the glass plates without being ground. Consequently, the X-ray diffraction data for O_2-annealed samples reflect the composition of the materials near the surface; the penetration

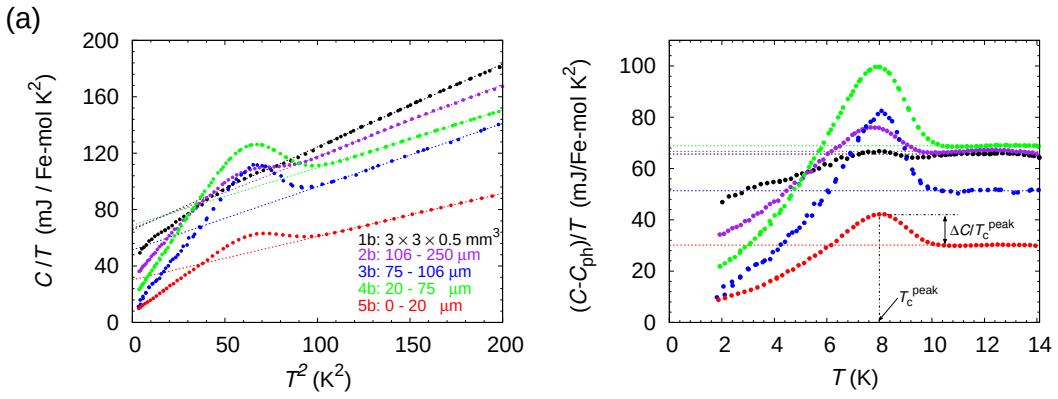

Fig. 2. (Color online) (a) C/T of O_2-annealed $Fe_{1.01}Te_{0.91}S_{0.09}$ against T^2 plot. (b) $(C - C_{ph})$ vs T plot of $Fe_{1.01}Te_{0.91}S_{0.09}$.

Table II. Parameters estimated by the specific heat measurements

Sample	size	β (mJ/K^{4}mol)	θ_D (K)	γ (mJ/Fe-mol K^2)	onset-T_c (K)	T_c^{peak} (K)	$\Delta C/T_c^{peak}$ (mJ/Fe-mol K^2)
1b	3 3 0.5 mm^3	0.59	149	66	(9.0)	(8.0)	-
2b	106 - 250 μm	0.51	156	67	9.5	7.8	9.3
3b	75 - 106 μm	0.45	163	51	9.6	8.1	31
4b	20 - 75 μm	0.41	169	69	10.2	8.0	31
5b	0 - 20 μm	0.31	185	30	10.0	8.0	12

depth of the X-ray used is about 5 μm. The data were scaled by the (101) peak intensity because of quite a high intensity of (00l) peaks owing to the O_2-annealed samples being naturally oriented. Figure 3(b) shows an enlarged view of the data for the as-grown sample and the smallest sample 5c. In the as-grown sample, small peaks from FeS and $FeTe_2$ are also seen in addition to the peaks of $Fe_{1.01}Te_{0.91}S_{0.09}$. Since sulfur has a solubility limit,[9] the surplus sulfur might react and form these impurities. Therefore, these impurities could be inevitable in the single crystalline sample grown by the self flux method. Besides this, the two peaks at 40.5° and 42.1° attributable to $FeTe_2$ are clearly observed for the O_2-annealed samples. $FeTe_2$ is probably generated by the O_2 annealing at surfaces of $Fe_{1.01}Te_{0.91}S_{0.09}$. $FeTe_2$ has been observed also in $Fe_{1+y}Te_{1-x}S_x$ annealed in the oxygen at temperatures higher than 300 °C.[11] For all of the samples annealed in oxygen atmosphere, reflections attributable to Fe_2O_3 or Fe_3O_4 were not observed. In the smallest powder sample 5c, many additional peaks were observed. Although they have not been identified, other impurity peaks indicated by arrows are also seen. Other unidentified materials are produced by O_2 annealing especially in the smallest sample 5c.

4. Discussion

The sample-size dependences of the SVF in O_2-annealed $Fe_{1.01}Te_{0.91}S_{0.09}$ evaluated from FC susceptibility and from specific heat measurements show almost the same trend as illustrated in Fig. 4. The SVF becomes greater with decreasing sample size down to 20 μm, but it becomes lower in smaller samples. The results indicate two types of effects of O_2 annealing in $Fe_{1.01}Te_{0.91}S_{0.09}$: creation and deterioration of superconducting regions. It is unable to evaluate the accurate SVF from these results because of the difficulty of the analysis for the specific heat as mentioned above. The volume fraction, however, may be roughly estimated to be dozens of percent of order by assuming the BCS theory, comparing $\Delta C/T_c^{peak}$ observed in sample 3b and 4b are from 0.4γ–0.6γ, which is 1.43γ in the BCS theory.

From the sample-size dependence of the superconducting volume fraction, the superconducting regions probably exist within a thickness of a few tens of micro meters from the surface. Figure 5 shows schematic diagrams of the O_2-annealing effects we propose. In order to construct these diagrams, we have made the following assumptions:

(1) O_2 annealing mostly affects regions close to sample surfaces.

(2) As a consequence of the O_2 annealing, two distinct layers are formed near the surfaces. The outer layer contains a large amount of non-superconducting materials such as $FeTe_2$ while the inner layer mostly consists of superconducting regions that encloses almost the whole sample. The core region surrounded by the two layers remains unchanged after the annealing.

(3) The thicknesses of those two layers are anisotropic due to the anisotropy of the crystal structure, but are independent of the sample size, and may be regarded as somewhat similar to a penetration depth of the annealing effects.

In fact, the formation of layers responsible for superconductivity,which enclose almost the whole sample, is consistent with the large difference between the SF in ZFC and FC conditions. Indeed, these assumptions reasonably well account for the observations concerning the SVF. The SVF will increase with decreasing sample size when the dimensions of the sample is considerably larger than the thickness of the two layers. On the other hand, when the dimensions of the sample becomes less than the thickness of the layers, the inner superconducting layer will naturally diminish and the SVF will decrease. As shown in Table II, the electronic specific heat coefficient γ of the sample class #5 is relatively small. This result is consistent with our view shown in Fig 5 because $FeTe_2$, which is an insulator ($\gamma \sim 0$), is one of the major impurities in the smallest sample class #5.[25] As stated earlier, the X-ray diffraction measurements did not detect oxidized iron such as Fe_2O_3 or Fe_3O_4 in the O_2-annealed samples. Nevertheless, we observed an oxygen component at surfaces of the O_2-annealed samples in EPMA measurements. We conjecture that oxygen could be diffused in $Fe_{1+y}Te_{1-x}S_x$ and intercalated between adjacent atomic layers as suggested in Ref.11. Such intercalation perhaps reduces the effects of excess iron and induces superconductivity.

5. Conclusions

We have investigated the sample-size dependence of the O_2-annealing effects by means of ZFC and the FC susceptibility and specific heat measurements. We observed a jump of the specific heat around superconducting transition temperature T_c in the O_2-annealed small samples. As far as we know, this is the first observation of the bulk superconductivity in

$Fe_{1+y}Te_{1-x}S_x$. It implies that the superconducting region induced by O_2 annealing is distributed probably near the surface of samples over a length of a few tens of micro meters in the annealing condition of 1 atm, 2 hours, and 200 °C.

Acknowledgements

This work was partly carried out under the Visiting Researcher's Program of the Institute for Solid State Physics, the University of Tokyo. We would like to thank H. Yoshizawa for his support in the specific heat measurements.

We are grateful to K. Motoya and T. Moyoshi for allowing us to use electron probe microanalyzer (EPMA) and equipment for sample synthesis.

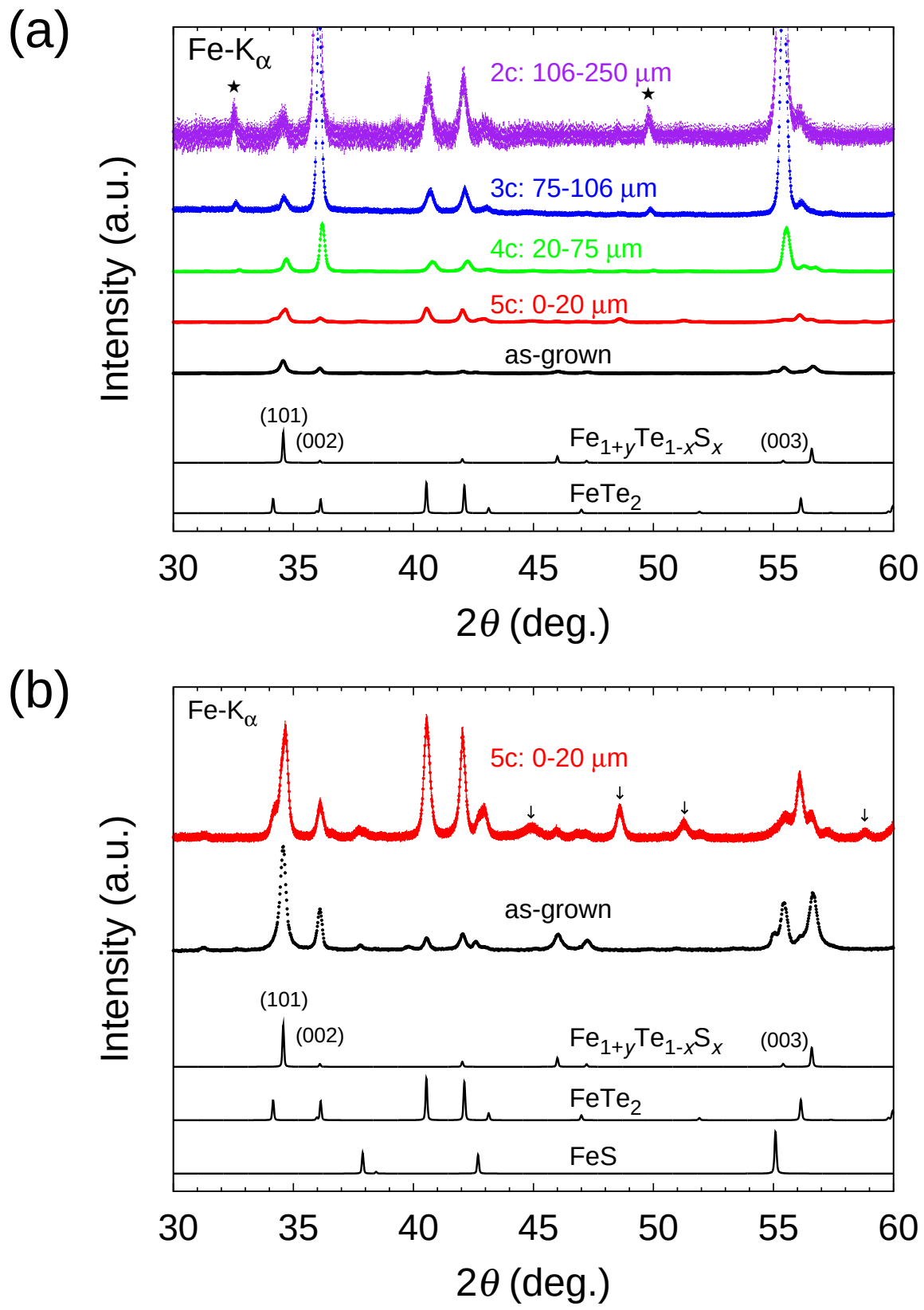

Fig. 3. (Color online) (a) X-ray powder diffraction patterns of size-classified O_2-annealed $Fe_{1.01}Te_{0.91}S_{0.09}$ and the as-grown sample. (b) Enlarged view of data for the smallest sample 5c and the as-grown sample. The data are scaled by the peak intensity of the (101) reflection. Calculated spectra for $Fe_{1-x}Te_{1-x}S_x$, $FeTe_2$,and FeS are attached. The cross marks represent the (00*l*) reflections of Fe-K_β radiation. The arrows represent peaks of other materials that could not be identified.

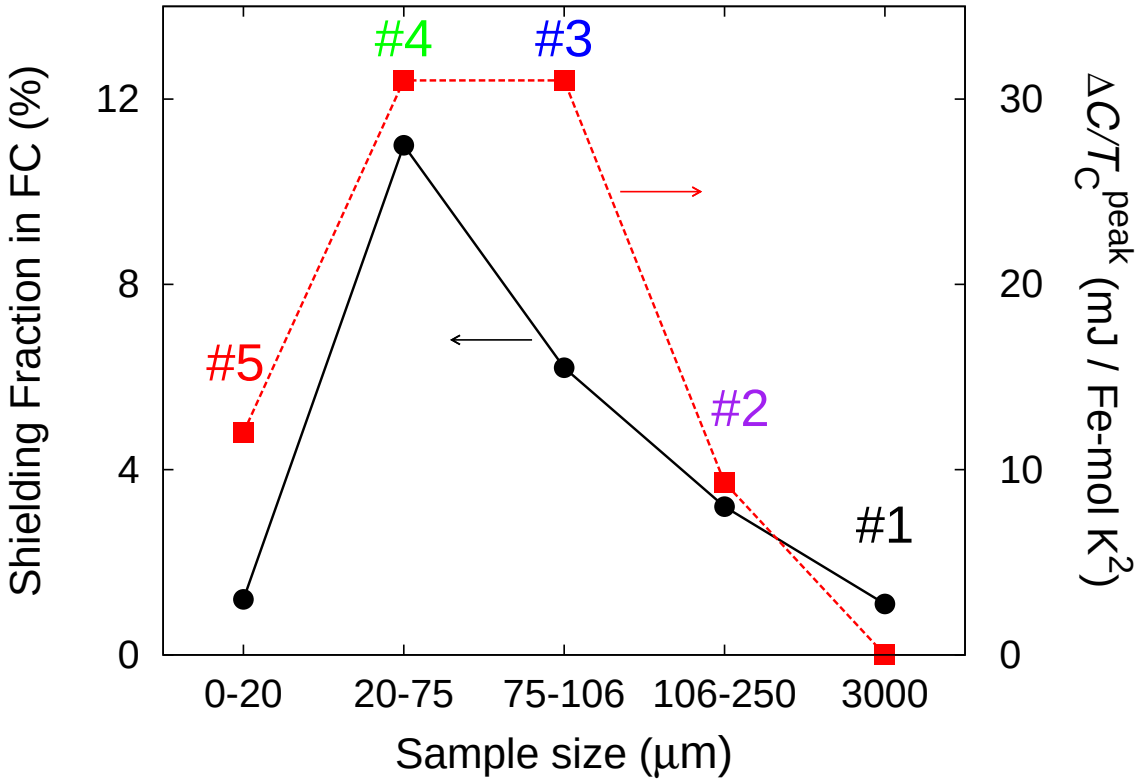

Fig. 4. (Color online) Sample size dependences of shielding fraction (SF) measured in FC condition and $\Delta C/T_{\mathrm{c}}^{\mathrm{peak}}$ evaluated from specific heat measurements.

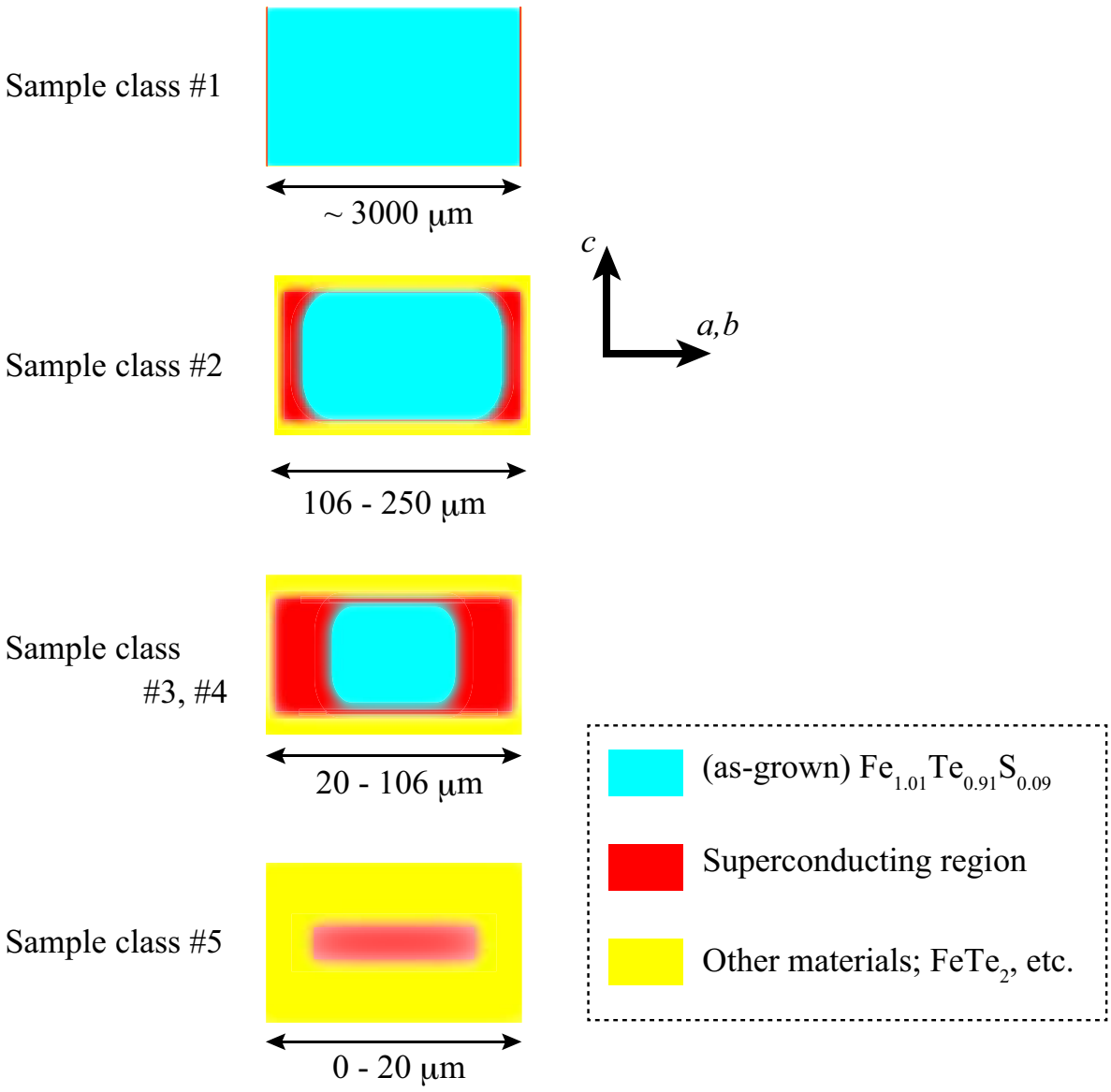

Fig. 5. (Color online) Schematic sectioned drawings of O_2-annealed $Fe_{1+y}Te_{1-x}S_x$. Assuming that the thickness of the superconducting region and that of the other produced materials region are fixed, the trend of the sample-size dependence of the superconducting volume fraction (SVF) can be explained.

References

1) Y. Kamihara, H. Hiramatsu, M. Hirano, R. Kawamura, H. Yanagi, T. Kamiya, and H. Hosono: J. Am. Chem. Soc. **128** (2006) 10012.
2) Y. Kamihara, T. Watanabe, M. Hirano, and H. Hosono: J. Am. Chem. Soc. **130** (2008) 3296.
3) K. Deguchi, Y. Takano, and Y. Mizuguchi: Sci. Technol. Adv. Mater. **13** (2012).
4) S. Li, C. de La Cruz, Q. Huang, Y. Chen, J. Lynn, J. Hu, Y.-L. Huang, F.-C. Hsu, K.-W. Yeh, M.-K. Wu, et al.: Phys. Rev. B **79** (2009) 054503.
5) W. Bao, Y. Qiu, Q. Huang, M. Green, P. Zajdel, M. Fitzsimmons, M. Zhernenkov, S. Chang, M. Fang, B. Qian, et al.: Phys. Rev. Lett. **102** (2009) 247001.
6) R. Hu, E. S. Bozin, J. Warren, and C. Petrovic: Phys. Rev. B **80** (2009) 214514.
7) P. Zajdel, P.-Y. Hsieh, E. E. Rodriguez, N. P. Butch, J. D. Magill, J. Paglione, P. Zavalij, M. R. Suchomel, and M. A. Green: J. Am. Chem. Soc. **132** (2010) 13000.
8) C. Koz, S. Rößler, A. A. Tsirlin, S. Wirth, and U. Schwarz: Phys. Rev. B **88** (2013) 094509.
9) Y. Mizuguchi, K. Deguchi, T. Ozaki, M. Nagao, S. Tsuda, T. Yamaguchi, and Y. Takano: Appl. Supercond. **21** (2011) 2866.
10) Y. Mizuguchi, K. Deguchi, S. Tsuda, T. Yamaguchi, and Y. Takano: Phys. Rev. B **81** (2010) 214510.
11) Y. Mizuguchi, K. Deguchi, S. Tsuda, T. Yamaguchi, and Y. Takano: Europhys. Lett. **90** (2010) 57002.
12) Y. Kawasaki, Y. Mizuguchi, K. Deguchi, T. Watanabe, T. Ozaki, S. Tsuda, T. Yamaguchi, and Y. Takano: Physica C **471** (2011) 611.
13) V. Awana, A. Pal, A. Vajpayee, B. Gahtori, and H. Kishan: Physica C **471** (2011) 77.
14) K. Deguchi, A. Yamashita, T. Yamaki, H. Hara, S. Demura, S. Denholme, M. Fujioka, H. Okazaki, H. Takeya, T. Yamaguchi, et al.: Journal of Applied Physics **115** (2014) 053909.
15) K. Deguchi, Y. Mizuguchi, Y. Kawasaki, T. Ozaki, S. Tsuda, T. Yamaguchi, and Y. Takano: Supercond. Sci. Technol. **24** (2011) 055008.
16) K. Deguchi, D. Sato, M. Sugimoto, H. Hara, Y. Kawasaki, S. Demura, T. Watanabe, S. Denholme, H. Okazaki, T. Ozaki, et al.: Supercond. Sci. Technol. **25** (2012) 084025.

17) T. Noji, M. Imaizumi, T. Suzuki, T. Adachi, M. Kato, and Y. Koike: J. Phys. Soc. Jpn. **81** (2012) 054708.

18) M. Imaizumi, T. Noji, T. Adachi, and Y. Koike: J. Phys.: Conf. Ser. **400** (2012) 022034.

19) Y. Kawasaki, K. Deguchi, S. Demura, T. Watanabe, H. Okazaki, T. Ozaki, T. Yamaguchi, H. Takeya, and Y. Takano: Solid State Commun. **152** (2012) 1135.

20) Y. Sun, T. Taen, Y. Tsuchiya, Z. Shi, and T. Tamegai: Supercond. Sci. Technol. **26** (2012) 015015.

21) E. E. Rodriguez, C. Stock, P.-Y. Hsieh, N. P. Butch, J. Paglione, and M. A. Green: Chemical Science **2** (2011) 1782.

22) Q. Shi, C. L. Snow, J. Boerio-Goates, and B. F. Woodfield: J. Chem. Therm. **42** (2010) 1107.

23) D. L. Martin: Can. J. Phys. **38** (1960) 17.

24) G. Chen, Z. Chen, J. Dong, W. Hu, G. Li, X. Zhang, P. Zheng, J. Luo, and N. Wang: Phys. Rev. B **79** (2009) 140509.

25) E. Westrum Jr, C. Chou, and F. Gronvold: J. Chem. Phys. **30** (1959) 761.